

Single photon nonlinearities using arrays of cold polar molecules

R. M. Rajapakse,¹ T. Bragdon,¹ A. M. Rey,² T. Calarco,³ and S. F. Yelin^{1,4}

¹*Department of Physics, University of Connecticut, Storrs, CT 06269*

²*JILA, National Institute of Standards and Technology and University of Colorado, Boulder, CO 80309-0440*

³*Institute for Quantum Information Processing, University of Ulm, D-89069 Ulm, Germany*

⁴*ITAMP, Harvard-Smithsonian Center for Astrophysics, Cambridge, MA 02138*

(Dated: May 3, 2022)

We model single photon nonlinearities via the dipole-dipole interactions of cold polar molecules. We propose utilizing "dark state polaritons" to effectively couple photon and molecular states; through this framework, coherent control of the nonlinearity can be expressed and potentially used in an optical quantum computation architecture. Due to the dipole-dipole interaction the photons pick up a measurable nonlinear phase even in the single photon regime. A manifold of protected symmetric eigenstates is used as basis. Depending on the implementation, major sources of decoherence result from non-symmetric interactions and phonon dispersion. We discuss the strength of the nonlinearity per photon and the feasibility of this system.

I. INTRODUCTION

Coherent control of optical nonlinearities at the single photon level is a burgeoning topic in quantum optics research. Utilizing state-preserving techniques, it is suggested [1, 2, 3, 4] that one can implement two-qubit quantum logic gates in a feasibly robust optical quantum computational framework.

Cold polar molecules are excellent candidates as a mediating medium due to their field-dependent intermolecular interaction properties [5, 6, 7]. They have been suggested for quantum computation architectures since they embody advantages of both neutral atoms and trapped ions, viz. long coherence times and strong interactions, respectively.

Advances in preparation (cooling and trapping) of molecular ensembles in their electronic, vibrational, and rotational ground states [8] would allow for single state manipulation in a characteristically rich level structure. Notably, recent work by Büchler et al. [9] predict novel, controllable superfluid and crystalline phase transitions from dipolar gases. The latter could suppress dephasing from short range collisions in high density traps. The anisotropic and long-range form of the dipole-dipole interaction is responsible for the bulk of advances in controlling molecular samples [5].

In this paper, we investigate cold polar molecular gases in one- and two-dimensional arrays. We describe single-photon nonlinearities resulting from the intermolecular dipole-dipole interaction. We applying Electromagnetically Induced Transparency (EIT) methodology for coherent state transfer. Next we calculate the resultant nonlinear phase in the context of collective excitations in an optically thick media.

Here we are primarily concerned with exploring feasibility of coherent control over the resultant nonlinear phase evolution of intermolecular dipole-dipole interactions. Familiar implementations for the system under discussion include stripline cavities, optical lattices, Wigner crystals, hollow fibers, or molecules on surfaces. Then,

we investigate the most significant decoherence effects for implementation in a trap architecture or crystalline phase.

II. SINGLE-PHOTON NONLINEARITY

Photons do not interact. However, "effective interactions" can be achieved by utilizing state-preserving light-matter couplings to nonlinear media, wherein matter-matter interactions effectuate photon-photon interactions without destroying the state information of the incident coherent fields.

The proposed mechanism is as follows: Photons are efficiently and coherently coupled into the molecular medium in the form of "slow-light polaritons." The molecule part of these light-molecule coupled excitations "switches" the zero-dipole rotational ground state into a high-dipole rotational superposition state. The resulting dipole-dipole interaction therefore adds a nonlinear phase to the polaritons that the photons retain on exiting the medium. We note that the nonlinear phase is thus proportional to the interaction time of the dipoles and thus the propagation time of the polaritons. Therefore control over the phase is exercised by manipulating the propagation velocity of the light in the medium.

EIT-based slow light polaritons [10, 11] are collective states of matter-light superposition that can be achieved by using a Λ -type system. Polaritons are the coupled exchanges of the signal field Ω_s and the superposed $|e\rangle$ and $|g\rangle$ ground states (see Fig. 1). $|g\rangle$ and $|e\rangle$ would typically be the $|J, M_J\rangle$ rotational states of the ground state molecules, where M_J is the projection on the z -axis of J . The coupling field Ω_c controls the slow group velocity of the polaritons.

The interacting states $|g\rangle$ and $|e\rangle$ in our system are the rotational levels of dipolar molecules. Since dipolar interactions exchange virtual photons, interacting states must have opposite parity. This can be accomplished via an expanded Λ -type system with a strong Raman transition involving a two-photon transition as Ω_c , or alternatively

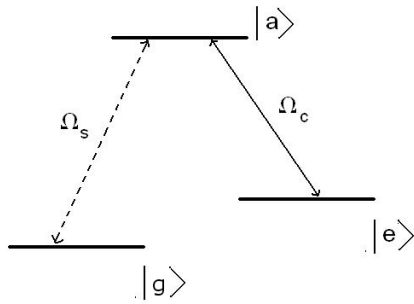


FIG. 1: Level scheme for utilizing slow-light polaritons. $|e\rangle$ and $|a\rangle$ can be coupled via a two-photon transition, or $|e\rangle$ can be a mixed parity state

the use of mixed-parity states for excited state $|a\rangle$. For simplicity we refer to the whole molecular system as an effective two-level system, consisting of $|e\rangle$ and $|g\rangle$, as is usually done in the context of slow-light polaritons [10]. We adopt a natural shorthand, $|g_i\rangle$ and $|e_i\rangle$ respectively for the ground and excited state of the i th molecule.

In our case, cold polar molecular gases constitute the nonlinear medium, e.g., SrO [1] or CaF [12]. The nonlinearity is expressed through dipole-dipole interactions, which depend functionally on the separation vector $\mathbf{r}_{ij} = \mathbf{r}_i - \mathbf{r}_j$ between dipoles $\boldsymbol{\mu}_i$ and $\boldsymbol{\mu}_j$ at sites i and j , respectively.

Let $|n\rangle$ be the short-hand notation for the corresponding n -photon effective dark state collective excitation. The resultant nonlinearity is then manifested for $n \geq 2$. Provided that each state $|n\rangle$ is an eigenstate of the molecule-field Hamiltonian, θ_n describes the nonlinear interaction phase evolution:

$$\hbar\theta_n(t) = \langle n | \hat{V}_{dd} t | n \rangle \quad (1)$$

where \hat{V}_{dd} is the dipole-dipole interaction potential, and therefore, we characterize the effective nonlinearity as

$$\Theta(t) = (\theta_2(t) - \theta_0(t)) - 2(\theta_1(t) - \theta_0(t)) = \theta_2 - 2\theta_1 + \theta_0 \quad (2)$$

For a linear medium this would be identical to zero. To fully characterize the nonlinearity we would have to include photon coupling states with $n > 2$, but in the scheme of optical quantum computation this is sufficient for a two-qubit controlled phase operation – provided appropriate single qubit gates.

We model an N molecule ensemble assuming collective excitation in a symmetric Dicke-like basis:

$$\begin{aligned} |0\rangle &= |g_1, \dots, g_N\rangle \\ |1\rangle &= \frac{1}{\sqrt{N}} \sum_{i=1}^N |g_1, \dots, e_i, \dots, g_N\rangle \\ |2\rangle &= \sqrt{\frac{2}{N(N-1)}} \sum_{i < j} |g_1, \dots, e_i, \dots, e_j, \dots, g_N\rangle \end{aligned} \quad (3)$$

For simplicity and to show the essential features of the dipole-dipole interaction, we assume that both $|g\rangle$ and $|e\rangle$ states are pure rotational states, which have zero dipole moment, and that the dipole-dipole interaction is governed by the $|g\rangle \leftrightarrow |e\rangle$ transition dipole moment. Formally, given a truncated basis for single molecules: $\mathbb{I}_i = |g_i\rangle\langle g_i| + |e_i\rangle\langle e_i|$ and that for purely rotational states, $\boldsymbol{\mu}_{gg} = \boldsymbol{\mu}_{ee} = 0$, we write the single molecule dipole moment operator:

$$\begin{aligned} \hat{\boldsymbol{\mu}}_i &= \boldsymbol{\mu}_{ge} |g_i\rangle\langle e_i| + \boldsymbol{\mu}_{eg} |e_i\rangle\langle g_i| \\ &\equiv \boldsymbol{\mu}_{ge} \hat{\sigma}_i^- + \boldsymbol{\mu}_{eg} \hat{\sigma}_i^+, \end{aligned} \quad (4)$$

with $\boldsymbol{\mu}_{ab} \equiv \mu_0 \langle a | \mathbf{e}_r | b \rangle$.

Assuming interacting dipoles are aligned and neglecting noncontributing terms $\hat{\sigma}_i^+ \hat{\sigma}_i^+$, $\hat{\sigma}_i^- \hat{\sigma}_i^-$, and arranging them in an array such that $\mathbf{r}_i \equiv z_i \hat{\mathbf{e}}_z$, the one-dimensional form of the interaction potential is

$$\hat{V}_{dd}^{(1D)} = \frac{-|\boldsymbol{\mu}_{eg}|^2}{4\pi\epsilon_0} \sum_{i < j} \frac{\hat{\sigma}_i^+ \hat{\sigma}_j^- + \hat{\sigma}_i^- \hat{\sigma}_j^+}{|z_i - z_j|^3}. \quad (5)$$

Upon exiting the medium, the signal field expresses the nonlinear effects of the medium proportional to the propagation time in the interacting medium as stated in Eqs. (1) and (2). Therefore, establishing a deterministic controlled phase operation is tantamount to exercising coherent control of the propagation and/or storage time of the polariton in the dipolar media. This corresponds to manipulating the control fields that establish the conditions for the “slow light” propagation.

Assuming periodic boundary conditions, e.g. a ring cavity, taken in the large N limit the nonlinear phase factor, Θ , is:

$$\Theta^{(1D)} \approx \frac{-2\kappa t \zeta[3]}{\hbar(N-1)} \quad (6)$$

where $\kappa \equiv \frac{-|\boldsymbol{\mu}_{eg}|^2}{4\pi\epsilon_0}$ and $\zeta[3] = \lim_{N \rightarrow \infty} \sum_{i=1}^{i=N-1} i^{-3} \approx 1.2$.

There is an optimization to undertake regarding the number of molecules in the array: On one hand, there must be enough molecules to create sufficient optical depth to couple-in the polaritons [13]. On the other hand, in order to maximize the nonlinearity in Eq. (6), less molecules are better.

Given aforementioned assumptions about dipole alignment, the two-dimensional lattice requires only a change of lattice vectors $\mathbf{r}_i = y_i \mathbf{e}_y + z_i \mathbf{e}_z$. We assume periodic boundary conditions and obtain

$$\Theta^{(2D)} \approx 2\Theta^{(1D)} \quad (7)$$

III. DECOHERENCE

a. Finite pulse effects

Slow light polaritons have linear dispersion in a linear medium through which phase coherence is maintained.

However, the nonlinear interaction in a simple 1D case adds a dispersion relation:

$$\hbar\omega_{k \rightarrow 0}^{1D} \rightarrow 2\kappa \left(2\zeta(3) + \left(-\frac{3}{2} + \ln k \right) k^2 + O(k)^3 \right) \quad (8)$$

where $E(k) = \hbar\omega_k$ describes the group dispersion in 1D. The constant part only rescales the resonance and the higher order terms can be mitigated by using long pulses or a (ring) cavity, where $k = 0$. In 2D the low energy excitations scale as

$$\hbar\omega_{k \rightarrow 0}^{2D} \rightarrow 6.55\kappa|\mathbf{k}| \quad (9)$$

b. Decay Out of Symmetric manifolds

Decay out of symmetric manifolds and phonon-like effects in Wigner crystal implementations can be significant. We will discuss symmetric manifolds at present, leaving the phonon-like decoherence effects to a later section.

Using angular momentum notation, $|j, m\rangle$, to describe rotational molecular ensemble states, we posit fully symmetric states with $j = N/2$ where $|m| \leq j$. Here $m = -N/2$ refers to the ensemble ground state, $|0\rangle$. The singly excited state $|1\rangle$ is equivalent to $m = -N/2 + 1$, and the doubly excited state $|2\rangle$ has $m = -N/2 + 2$. These states are a good basis if the relevant Hamiltonian is spherically symmetric.

V_{dd} , however, is not a spherically symmetric Hamiltonian, and therefore states with identical j but different m values are no longer degenerate. Further mixing emerges with the addition of the $j = N/2 - 2$ manifold for $|2\rangle$. Therefore the state changes over time and decoherence is accrued.

We have to consider the decay probability from an initial Dicke eigenstate we write as $|\psi_0(0)\rangle$ (where $|\psi(t=0)\rangle = |\psi_0(0)\rangle$) into a time evolved state $|\psi(t)\rangle = -\frac{i}{\hbar}V_{dd}|\psi_0(t)\rangle$, explained by using the fidelity $\mathcal{F}_0(t)$

$$\mathcal{F}_0(t) = |\langle \psi(t) | \psi_0(0) \rangle|^2. \quad (10)$$

This quantity is plotted for two different 1D sample sizes for a state with two excitations ($|2\rangle$) in Fig. 2. We observe that a phase gate can be realized when $\Theta(t) = \Theta(t_\pi) = \pi$,

One could effectively remove the mixture of j manifolds, each of which otherwise contributes to spontaneous decoherence by the addition of an external electric field. The following procedure generally establishes Many-body Protected Manifolds (MPM) [14], and would eliminate or mitigate this decoherence effect.

c. Phonon-like effects

In a Wigner crystal implementation, there exists another notable decoherence effect, which can be analyzed

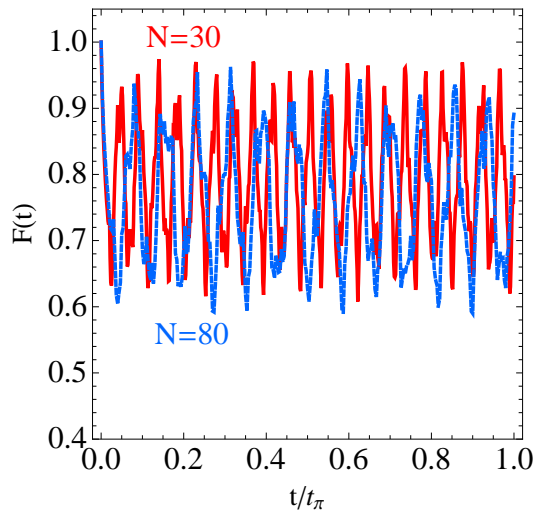


FIG. 2: Probability of decay out of a symmetric manifold for a state with two excitations $|2\rangle$, for sample sizes of 30 (red) and 80 (blue, dashed) molecules in 1D.

using a phonon formalism, [15]. In a realistic crystalline phase, the molecules are not fixed frozen. It is obvious that the phonon-like effects will add to the decay described in the previous section as their energy provides a coupling between the symmetric and non-symmetric states. Details of decoherence due to phonons will be treated in subsequent sections.

IV. MANYBODY PROTECTED MANIFOLDS

As the next step, we include a tunable DC electric field which thereby induces a dipole moment in the ground and excited states of the molecule ($\mu_{gg}, \mu_{ee} \neq 0$). This effect then augments the dipole-dipole interaction among our collective Dicke-like states in a way that enables perturbative treatment of the non-spherically symmetric part of the interaction, thus reinstating $|j, m\rangle$ as good eigenstates for the system:

$$\hat{V} + = H_H + H_I = \quad (11)$$

$$= \kappa \sum_{i < j} \frac{\hat{\sigma}_i \cdot \hat{\sigma}_j}{|\mathbf{r}_i - \mathbf{r}_j|^3} - \xi \sum_{i < j} \frac{\hat{\sigma}_i^z \hat{\sigma}_j^z}{|\mathbf{r}_i - \mathbf{r}_j|^3},$$

$$\text{where } \xi = \frac{\mu_{eg}^2 - \frac{1}{2}(\mu_{ee} - \mu_{gg})^2}{4\pi\epsilon_0}.$$

Here H_H is the spherically symmetric (Heisenberg) part of the Hamiltonian V , and H_I is the non-symmetric (Ising) part.

The relative strength of the H_H and H_I parts of \hat{V} can be manipulated to find values of ξ/κ such that MPM protection is maximized. For example, SrO has a $^1\Sigma$ ground state with a magnetic moment of 8.89D. Upon selecting ground and excited rotational states with opposing parity, the appropriate values of ξ and κ are then obtained

by diagonalizing the Stark Hamiltonian for variable electric fields [15]. It is noted that opposite parity states, or mixed parity states, are necessary for the dipole-dipole interaction to occur. In Fig. 3, we show the ratio of ξ/κ for varying DC field strength between two rotational levels of SrO. For induced dipole transitions, the biasing electric DC field E depends on both the rotational constant B and the ground state dipole moment μ_0 .

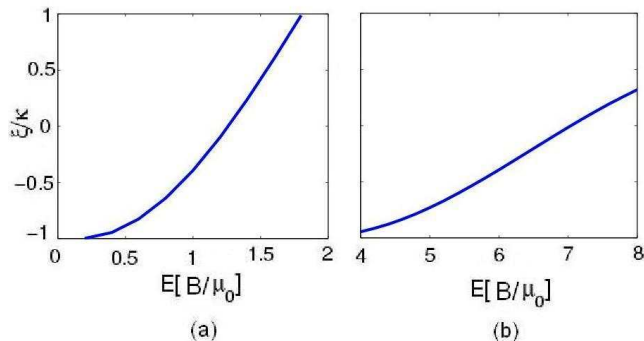


FIG. 3: ξ/κ for varying $E[B/\mu_0]$ in SrO. (a) $|g_i\rangle = |J_{\text{SrO}}, M_{J,\text{SrO}}\rangle = |0, 1\rangle_i$ and $|e_i\rangle = |1, 0\rangle_i$. (b) $|g_i\rangle = |1, 0\rangle_i$ and $|e_i\rangle = |2, 0\rangle_i$. B is the rotational constant of the molecule, and μ_0 is the maximum ground state dipole-moment, in our case assumed to be $\mu_0 = |\mu_{eg}|$.

The application of an electric field changes the original bare states to dressed states $|g\rangle$ and $|e\rangle$ which are linear superpositions of the bare states. It has to be noted that the addition of a DC field, leading to MPM protection, causes the nonlinearity to be reduced by a factor of $|\xi/\kappa|$.

a. Decay Out of Manybody Protected manifolds into other manifolds

In this section we study what occurs if at time $t = 0$ we prepare the system in the $j = N/2$ subspace and let the system evolve in time in the presence of MPM. This can be written as

$$|\Psi_n(t)\rangle = e^{-\frac{1}{2}\gamma_n(t)t} e^{-i\theta_n(t)} |N/2, -N/2 + n\rangle \quad (12)$$

Here we estimate the decay constants γ_n . Our objectives are to keep θ_n large while minimizing γ_n . As the states with 0 and 1 excitations are eigenstates of the symmetric manifold there is no decay out of the manifolds and therefore $\gamma_0 = 0$ and $\gamma_1 = 0$.

Using first-order perturbation theory we can write

$$e^{-\gamma_2(t)t} \simeq 1 - \frac{1}{\hbar} \sum_{\mathbf{k}, \mathbf{k}' > 0} \left| \int_0^t d\tau \mathcal{M}_{\mathbf{k}, \mathbf{k}'} e^{i\tau(\omega_{\mathbf{k}} + \omega_{\mathbf{k}'})} \right|^2 \quad (13)$$

where the matrix element $\mathcal{M}_{\mathbf{k}, \mathbf{k}'} = \langle N/2, -N/2 + 2 | \hat{H}_I | \psi_{\mathbf{k}, \mathbf{k}'} \rangle$. Here, \hat{H}_I is the perturbative part of \hat{V} which is $\hat{H}_I = -\xi \sum_{i,j; i \neq j} \frac{\hat{\sigma}_i^z \hat{\sigma}_j^z}{|\mathbf{r}_i - \mathbf{r}_j|^3}$.

Here \mathbf{k}, \mathbf{k}' are the wave vectors of the two excitations. If $\mathbf{k}' = 0$, then $\psi_{\mathbf{k}, 0}$ is a Dicke state. However when $\mathbf{k}, \mathbf{k}' > 0$, $\psi_{\mathbf{k}, \mathbf{k}' > 0}$ is a time evolved state that is not part of the Dicke manifold, as the decay out of the manifold is caused by the scattering of the two excitations by each other.

Thus we obtain $\mathcal{M}_{\mathbf{k}, \mathbf{k}'} = \frac{4\xi}{N} F_{\mathbf{k}} \delta_{\mathbf{k}, -\mathbf{k}'}$ where $F_{\mathbf{k}}$ is the Fourier series of $|r_i - r_j|^{-3}$, i.e. $F_{\mathbf{k}} = \sum_j |r_0 - r_j|^{-3} \cos(\mathbf{k} \cdot \mathbf{r}_j^0)$. Replacing this expression in Eq. (13) yields

$$e^{-\gamma_2(t)t} \simeq 1 - \frac{16\xi^2}{N^2} \sum_{\mathbf{k} > 0} |F_{\mathbf{k}}|^2 \frac{\sin^2(\omega_{\mathbf{k}} t)}{\hbar^2 \omega_{\mathbf{k}}^2}. \quad (14)$$

As the interaction time t grows linearly with N we are interested in the behavior when t is large.

We solve the exact many-body dynamics numerically by evolving a system initially prepared in the Dicke state with $m = -N/2 - 2$ under the effective Hamiltonian \hat{V} , and compute the fidelity, \mathcal{F} of remaining in a Dicke state:

$$\mathcal{F}(t) = \left| \langle N/2, -N/2 + 2 | \Psi(t) \rangle \right|^2 = e^{-\gamma_2(t)t}. \quad (15)$$

We can compare the results we obtained from Eq. (15) to that obtained from Eq. (10). In Fig. 4 we solve for the 1D dynamics using the parameters $\xi/\kappa = 0.05$ and $N = 36$ and 81. The grid line is at t_π , the time when we reach the required phase. t_π should also occur when decay probability is at a minimum; this can be achieved by adjusting the parameters of the system. Fig. 4 confirms the prediction that in 1D the fidelity decreases with increasing N . Fig. 5 emphasizes the gain in fidelity obtained by going from 1D to 2D [16]. With the same number of molecules and even a much larger $\xi/\kappa = 1$ the fidelity is much better than in 1D. We find that for moderate N the 1D decay probability increases as $\approx 0.01 \frac{\xi^2}{\kappa^2} N^{1.62}$, which is obtained via a fit. This relation implies that in order to implement a robust gate

$$\frac{\xi^2}{\kappa^2} \ll \frac{100}{N^{1.62}} \quad (16)$$

However, by choosing ξ/κ small we pay the price of having slower dynamics and therefore we make the system more vulnerable to other type of loss.

V. WIGNER CRYSTAL AND PHONONS

In dense systems with sufficiently strong fixed DC electric fields, [9], one can realize a crystalline phase of polar molecules thereby forming a Wigner crystal. In this phase, molecules are not fixed frozen, but instead oscillate about an equilibrium position, \mathbf{r}_i^0 . These oscillations can be described using phonon formalism [15]. The phonon spectrum is continuous with no energy gap. Therefore, if we rewrite the molecular position operators

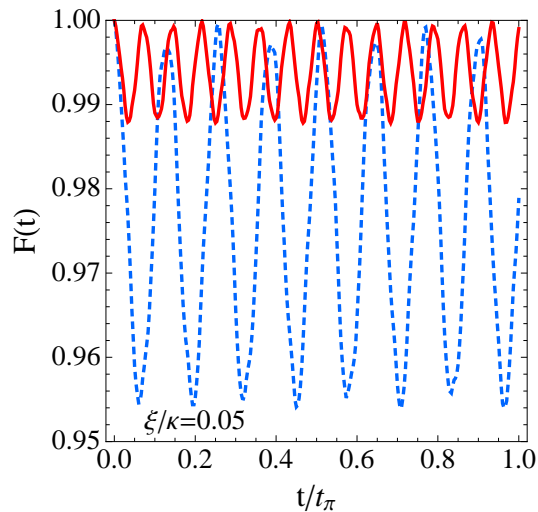


FIG. 4: 1D system: Fidelity of remaining in the Dicke state with two excitations during the time evolution. The blue (dashed) and red lines are the solutions of Eq. (13) for $n=81$ and $n=36$, respectively. The ratio of $\xi/\kappa = 0.05$ gives oscillatory behavior. Larger values of ξ/κ give lesser fidelity.

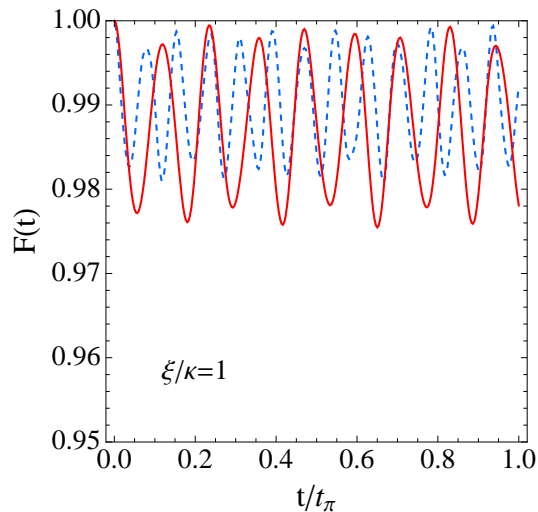


FIG. 5: 2D system: Fidelity of remaining in the Dicke state with two excitations during the time evolution. The blue (dashed) and red lines are the solutions of Eq. (13) for $n=81$ and $n=36$, respectively. The ratio of $\xi/\kappa = 1$ gives oscillatory behavior, and no longtime decay out of the manifolds.

as $\mathbf{r}_i = \mathbf{r}_i^0 + \mathbf{x}_i$ to account for small fluctuations around the equilibrium position \mathbf{r}_i^0 and expand V_{dd} in powers of \mathbf{x}_i we obtain terms for phonon-polariton interactions. We can describe the dynamics of the the coupling between phonons and polaritons which is given by the Hamiltonian V_{phon}

$$V_{phon} = -\kappa \sum_{i \neq j} G_{ij} \vec{\sigma}_i \cdot \vec{\sigma}_j - \xi \sum_{i \neq j} G_{ij} \sigma_i^z \sigma_j^z + 4B_0 \sum_{i \neq j} G_{ij} (\sigma_i^z + \sigma_j^z), \quad (17)$$

where

$$G_{ij} = -3a^3 \frac{(\mathbf{x}_i - \mathbf{x}_j) \cdot (\mathbf{r}_i^0 - \mathbf{r}_j^0)}{4|\mathbf{r}_i^0 - \mathbf{r}_j^0|^5}.$$

and $B_0 = (\mu_{ee}^2 - \mu_{gg}^2)/2$.

If at time $t = 0$ we prepare our state in the $J = N/2$ manifold, the projection of the evolving state on the symmetric manifold can then be written as

$$|\Psi_n(t)\rangle = e^{-\frac{\gamma_{n,ph}(t)}{2}t} e^{-i\theta_n(t)} |N/2, -N/2 + n\rangle. \quad (18)$$

The decoherence rates γ_{1ph} and γ_{2ph} can be approximately calculated using perturbation theory [15], where $N(x) = 1/(e^{\hbar x/(kBT)} - 1)$ is the thermal occupation number for phonons with the phonon spectrum $\omega_\lambda(\mathbf{q})$ (see Fig. 8 and Fig. 9) and $\Omega_{q,k,\lambda}^\pm = \omega_\lambda(\mathbf{q}) \pm E(k)/\hbar$, $E(k) = \hbar\omega_k$ is the group dispersion.

This yields an expression for γ_{1ph} that can be given by:

$$\gamma_{1ph} \simeq \frac{\pi(\xi + 4B_0)^2}{\hbar\sqrt{\Gamma}} \sum_\lambda \int \frac{d^D(\mathbf{a}\mathbf{k})}{(2\pi)^D} g_\lambda(\mathbf{k}) [(N(\omega_\lambda(\mathbf{k})) + 1)\delta(\omega_\lambda(\mathbf{k}) - \omega_{\mathbf{k}}) + N(\omega_\lambda(\mathbf{k}))\delta(\omega_\lambda(\mathbf{k}) + \omega_{\mathbf{k}})]. \quad (19)$$

For two photon excitations it can be shown in a similar way that

$$\gamma_{2ph} \approx 2\gamma_{1ph}. \quad (20)$$

Detailed derivations are included in App. B.

In [15] analytical expressions for the decay rates in the thermodynamic limit were derived using the Fermi Golden Rule. In this limit the decoherence induced by phonons was only relevant in 1D and proportional to the temperature. For our finite number of molecules Fermi Golden rule results are not valid and the results are summarized in Fig. 6 and Fig. 7. In Fig. 6 and Fig. 7 we plot the time evolution of the decay probability for two systems with different N . There is a general tendency of the maximum decay probability to grow linearly with N for both 1D and 2D. Also for fixed N , Γ and κ we observe a linear dependence on the temperature that can also be predicted by the Fermi Golden Rule.

VI. CONCLUSION

In this paper, we explore the feasibility of utilizing cold polar molecules in 1D and 2D optical lattices for coherently controlled nonlinear optics. Specifically, we address the major decoherence effects of non-symmetric interactions and finite pulse dispersion. For crystalline samples, we have explored phonon-induced effects.

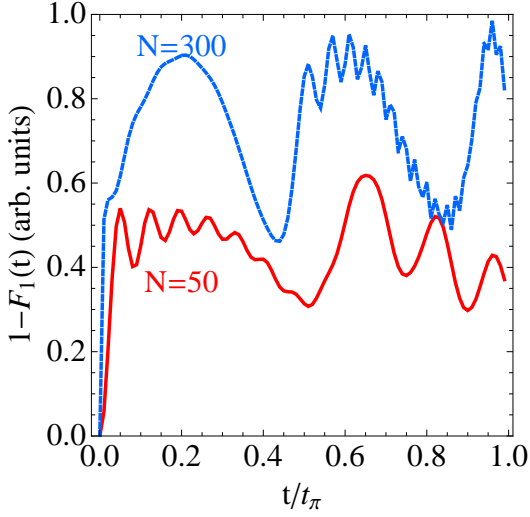


FIG. 6: $1 - F_1(t)$, where $1 - F_1(t)/(\xi + 4B_0)^2/\sqrt{\Gamma}$ is the probability of decay of a single excitation for a 1D system with $N = 36$ (red), $N = 80$ (blue, dashed) and ξ , B_0 and Γ are system dependant parameters.

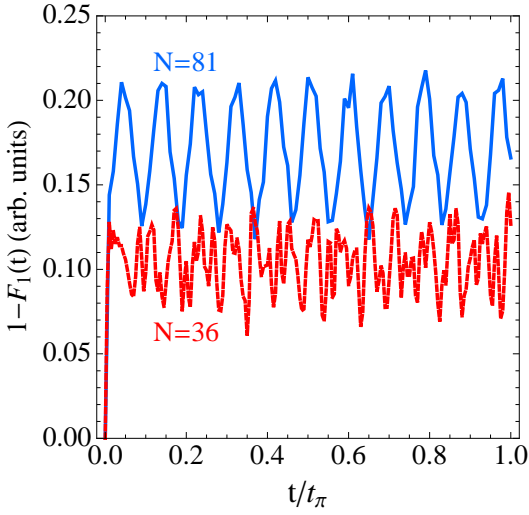


FIG. 7: $1 - F_1(t)$, where $1 - F_1(t)/(\xi + 4B_0)^2/\sqrt{\Gamma}$ is the probability of decay of a single excitation for a 2D system with $N = 36$ (red), $N = 80$ (blue, dashed) and ξ , B_0 and Γ are system dependant parameters.

We report a controlled π phase gate time that increases proportionally to the number of interacting systems, but also note better fidelity in 2D systems for reasonable system parameters and external field strengths. Using optical cavities or ring lattices the robustness of the gate operation can be further improved. Furthermore, in the crystalline phase, spin echo techniques could reduce long wave phonon excitations to maximize nonlinear response.

Acknowledgments

The authors wish to acknowledge NSF for funding, and Peter Rabl for fruitful discussions. Tommaso Calarco wishes to acknowledge the EC Integrated Project SCALA.

Appendix A

1. Decay of a single excitation

We start by deriving the decoherence rate γ_{1ph} for single excitations. To first order in perturbation theory we can write

$$e^{-\gamma_{1ph}(t)} \simeq 1 - \frac{2}{\hbar^2} \int_0^t dt' \int_0^{t'} d\tau \sum_{\mathbf{q}, \lambda, \mathbf{k} > 0} |\mathcal{L}_{\mathbf{k}, \mathbf{q}, \lambda}|^2 \cdot \left[(N(\omega_\lambda(\mathbf{q})) + 1) \cos(\Omega_{\mathbf{q}, \mathbf{k}}^+ \tau) + N(\omega_\lambda(\mathbf{q})) \cos(\Omega_{\mathbf{q}, \mathbf{k}}^- \tau) \right], \quad (21)$$

where $N(\omega) = 1/(e^{\hbar\omega/(k_B T)} - 1)$ is the thermal occupation number for phonons with the phonon spectrum $\omega_\lambda(\mathbf{q})$ and $\Omega_{\mathbf{q}, \mathbf{k}}^\pm = \omega_\lambda(\mathbf{q}) \pm E(k)$. Here $\omega_\lambda(q)$ is the frequency of a phonon with wave number q and λ labels the two phonon branches in 2D. (see Fig.8 and Fig.9). $E(k)$ is the dispersion relation of a polariton with wave number k (Eq. (8)).

In deriving the exact form of $\mathcal{L}_{\mathbf{k}, \mathbf{q}, \lambda}$, we first write V_{phon} as in Eq. (17) and thus obtain the form of $\mathcal{L}_{\mathbf{k}, \mathbf{q}, \lambda}$ as

$$\begin{aligned} \mathcal{L}_{\mathbf{k}, \mathbf{q}, \lambda} &= \left| \langle \psi_0 | V_{phon} | \psi_k \rangle \right| \\ &= \sum_{ij} \left| \langle \psi_0 | -\kappa \sum_{i \neq j} G_{ij} \vec{\sigma}_i \cdot \vec{\sigma}_j \right. \\ &\quad \left. - \xi \sum_{i \neq j} G_{ij} \sigma_i^z \sigma_j^z + 4B_0 \sum_{i \neq j} G_{ij} (\sigma_i^z + \sigma_j^z) | \psi_k \rangle \right| \end{aligned} \quad (22)$$

We can rewrite $\mathcal{L}_{\mathbf{k}, \mathbf{q}, \lambda}$, with only the perturbative terms as

$$\begin{aligned} \mathcal{L}_{\mathbf{k}, \mathbf{q}, \lambda} &= -3 \sqrt{\frac{1}{2N\sqrt{\Gamma} f_\lambda(\mathbf{q})}} \sum_{i,j} \frac{a^4 (\mathbf{e}_\lambda \cdot (\mathbf{r}_i^0 - \mathbf{r}_j^0))}{4|\mathbf{r}_i^0 - \mathbf{r}_j^0|^5} \\ &\quad \left[e^{i\mathbf{q} \cdot \mathbf{r}_i^0} \langle \psi_0 | -\xi \sigma_i^z \sigma_j^z + 4B_0 (\sigma_i^z + \sigma_j^z) | \psi_k \rangle \right] \end{aligned} \quad (23)$$

where $f_\lambda(\mathbf{q}) = \sqrt{\Gamma} \omega_\lambda(\mathbf{q})$, and Γ is the ratio between the interaction and kinetic energies. With the substitution of

$$g_\lambda(\mathbf{q}) \equiv \frac{9}{f_\lambda(\mathbf{q})} \left(\sum_{i \neq 0} \left[\sin(\mathbf{q} \cdot \mathbf{r}_i^0) \frac{(a^4 \mathbf{e}_\lambda \cdot \mathbf{r}_i^0)}{|\mathbf{r}_i^0|^5} \right] \right)^2$$

Eq. (23) can be rewritten as:

$$\mathcal{L}_{\mathbf{k},\mathbf{q},\lambda} = i\sqrt{\frac{1}{2N\sqrt{\Gamma}}}(\xi + 4B_0)\delta_{\mathbf{q},-\mathbf{k}}\sqrt{g_\lambda(\mathbf{q})} \quad (24)$$

In the regime where the Fermi Golden Rule is expected to be valid the decay rate is constant; $\gamma(t) = \gamma$ and using Eq. (26) and the properties of Dirac delta functions can be given by

$$\begin{aligned} \gamma_{1ph} &\simeq \frac{\pi(\xi + 4B_0)^2}{\hbar\sqrt{\Gamma}} \\ &\sum_{\lambda} \int \frac{d^D(\mathbf{a}\mathbf{k})}{(2\pi)^D} g_\lambda(\mathbf{k}) [(N(\omega_\lambda(\mathbf{k})) + 1)\delta(\omega_\lambda(\mathbf{k}) - \omega_{\mathbf{k}}) \\ &+ N(\omega_\lambda(\mathbf{k}))\delta(\omega_\lambda(\mathbf{k}) + \omega_{\mathbf{k}})]. \end{aligned} \quad (25)$$

D is the number of dimensions and $\omega_{\mathbf{k}} = E(k)/\hbar$.

2. Decay of two dipolar excitations

In the main body of our paper we have stated that $\gamma_{2ph} \approx 2\gamma_{1ph}$. A detailed derivation is given below.

To first order in perturbation theory we can write

$$\begin{aligned} e^{-\gamma_{1ph}(t)} &\simeq 1 - \frac{2}{\hbar^2} \int_0^t dt' \int_0^{t'} d\tau \sum_{\mathbf{q},\lambda,\mathbf{k}>0} |\mathcal{L}_{\mathbf{k},\mathbf{q},\lambda}|^2 \\ &[(N(\omega_\lambda(\mathbf{q})) + 1) \cos(\Omega_{\mathbf{q},\mathbf{k}}^+ \tau) + N(\omega_\lambda(\mathbf{q})) \cos(\Omega_{\mathbf{q},\mathbf{k}}^- \tau)], \end{aligned} \quad (26)$$

Where $\Omega_{\mathbf{q},\mathbf{k},\mathbf{k}'}^\pm = \omega_{\lambda(\mathbf{q})} \pm E(k)/\hbar \pm E(k')/\hbar$. $\mathcal{S}_{\mathbf{k},\mathbf{k}',\mathbf{q},\lambda}$ is rewritten in the same form as

$$\begin{aligned} \mathcal{S}_{\mathbf{k},\mathbf{k}',\mathbf{q},\lambda} &= -3\sqrt{\frac{1}{2N\sqrt{\Gamma}f_\lambda(\mathbf{q})}} \\ &\sum_{ij} [e^{i\mathbf{q}\cdot\mathbf{r}_i^0} \langle \psi_0 | -\xi\sigma_i^z \sigma_j^z \\ &+ 4B_0(\sigma_i^z + \sigma_j^z) | \psi_{\mathbf{k},\mathbf{k}'} \rangle \frac{a^4(\mathbf{e}_\lambda \cdot (\mathbf{r}_i^0 - \mathbf{r}_j^0))}{4|\mathbf{r}_i^0 - \mathbf{r}_j^0|^5}] \\ &= 3i\sqrt{\frac{1}{2N\sqrt{\Gamma}f_\lambda(\mathbf{q})}} ((\xi + 4B_0)(\delta_{\mathbf{q},-\mathbf{k}}\delta_{\mathbf{k}',\mathbf{0}} + \\ &\delta_{\mathbf{q},-\mathbf{k}'}\delta_{\mathbf{k},\mathbf{0}}) - \frac{4\xi}{N}\delta_{-\mathbf{q},\mathbf{k}+\mathbf{k}'}) \\ &\times \sum_{i \neq 0} \left[\sin(\mathbf{q} \cdot \mathbf{r}_i^0) \frac{(a^4 \mathbf{e}_\lambda \cdot \mathbf{r}_i^0)}{|\mathbf{r}_i^0|^5} \right] \end{aligned} \quad (27)$$

In the above expression the term proportional to ξ/N is much smaller than the one proportional to $\xi + 4B_0$ and can be neglected. Under this assumption, $\gamma_{2ph}(t) \rightarrow \gamma_{2ph}$,

$$\gamma_{2ph} \approx 2\gamma_{1ph} \quad (28)$$

Appendix B

By single excitations we refer to states with $M = -N/2 + 1$ and $J = N/2 - 1$. There are $N - 1$ different states, i.e $k = 1, \dots, N - 1$.

$$|\psi_{\mathbf{k}}\rangle = \frac{1}{\sqrt{N}} \sum_j e^{i\mathbf{k}\cdot\mathbf{r}_j^0} \sigma_j^+ |N/2, -N/2\rangle \quad (29)$$

are eigenstates of the Hamiltonian.

The phonon spectrum for 2D states is given in Fig. 9.

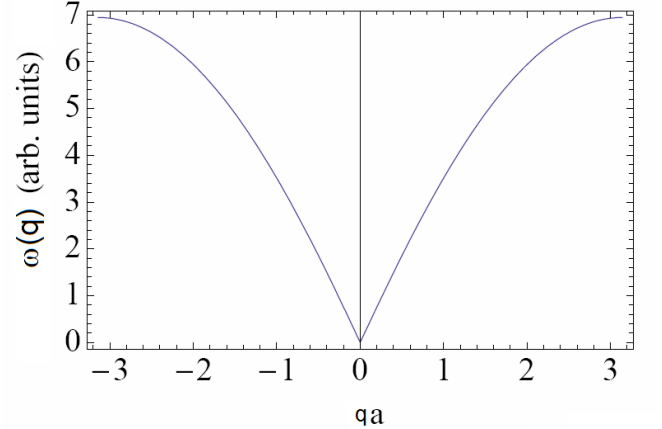


FIG. 8: Phonon excitation spectrum in 1D for a single excitation. a is the separation between the molecules. The units of $\omega(q)$ are $ma^2\sqrt{\Gamma}$

[1] D. Demille, Phys. Rev. Lett. **88**, 067901 (2002).

[2] C. Lee and E. A. Ostrovskaya, Phys. Rev. A **72**, 062321 (2005).

[3] M. D. Lukin, M. Fleischhauer, R. Côté, L. M. Duan, D. Jaksch, J. I. Cirac, and P. Zoller, Phys. Rev. Lett. **87**, 037901 (2001).

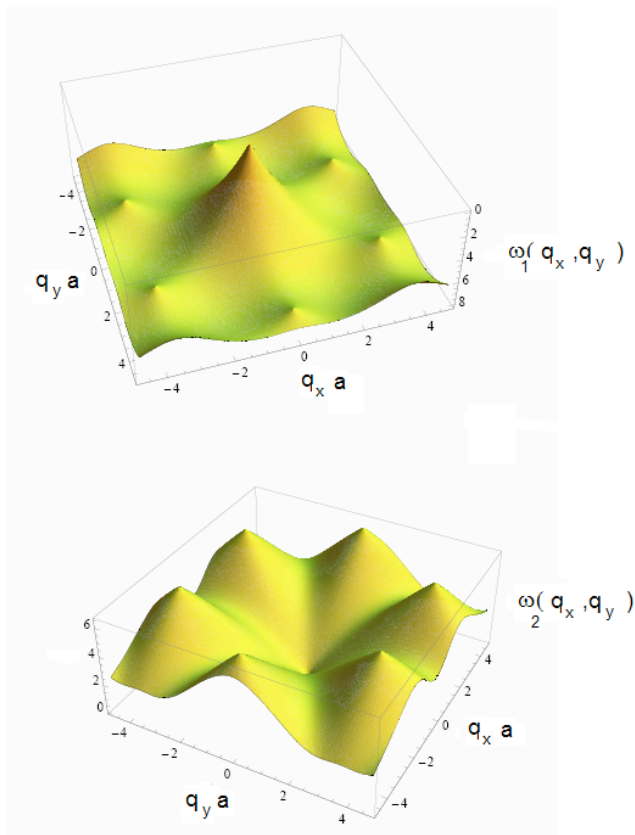


FIG. 9: Phonon Excitation spectrum in 2D for the two different branches of the phonon spectrum. q_x and q_y label the two quasimomenta, and $\omega(q)$ is the frequency of the phonons. The units of $\omega_1(q_x, q_y)$ are $ma^2\sqrt{\Gamma}$

- [4] I. Friedler, D. Petrosyan, M. Fleischhauer, and G. Kurizki, Phys. Rev. A **72**, 043803 (2005).
- [5] D. Jaksch, H. J. Briegel, J. I. Cirac, C. W. Gardiner, and P. Zoller, Phys. Rev. Lett. **82**, 1975 (1999).
- [6] A. Andre, J. M. Doyle, D. DeMille, M. D. Lukin, S. E. Maxwell, and P. Rabl, Nature Phys. **2**, 636 (2006).
- [7] S. F. Yelin, K. Kirby, and R. Cote, Phys. Rev. A **94**, 050301 (2006).
- [8] K.-K. Ni, S. Ospelkaus, M. H. G. de Miranda, A. Pe'er, B. Neyenhuis, J. J. Zirbel, S. Kotochigova, P. S. Julienne, D. S. Jin, and J. Ye, Science **322**, 231 (2008).
- [9] H. P. Büchler, E. Demler, M. Lukin, A. Micheli, and P. Zoller, Phys. Rev. Lett. **98**, 060404 (2007).
- [10] M. Fleischhauer and M. D. Lukin, Phys. Rev. Lett. **84**, 5094 (2000).
- [11] M. Lukin, Rev. Mod. Phys. **75**, 457 (2003).
- [12] A. Micheli, G. Pupillo, H. P. Büchler, and P. Zoller, Phys. Rev. A **76**, 043604 (2007).
- [13] M. Bajcsy, S. Hofferberth, V. Balic, T. Peyronel, M. Hafezi, A. S. Zibrov, V. Vuletic, and M. Lukin (2009), arxiv: 0901.0336v1.
- [14] A. M. Rey, L. Jiang, M. Fleischhauer, E. Demler, and M. Lukin, Phys. Rev. A **77**, 052305 (2008).
- [15] P. Rabl and P. Zoller, Phys. Rev. A **76**, 042308 (2007).
- [16] For simplicity we assumed a square lattice. This assumption does not change the overall picture of the dynamics if one looks at other types of 2D lattices, such as triangular ones.